MEDICAL PHYSICS' LEADING QA SOFTWARE JUST GOT EVEN BETTER.

THE RIT FAMILY OF PRODUCTS VERSION 6.10

UTILIZE RIT'S INNOVATIVE UPDATE FOR THE MOST ADVANCED QA CAPABILITIES

NEW FEATURE HIGHLIGHTS INCLUDE:

Isocenter Optimization with Angle Flexibility

RIT's popular 3D Winston-Lutz routine offers expanded flexibility with customizable angle configurations. These reduced requirements allow you to mimic more clinically relevant angles for determining isocenter at specific treatment configurations. The routine also features a new couch walkout plot (beam deviation vs. the couch rotation angle) and detailed annotations with routine information.

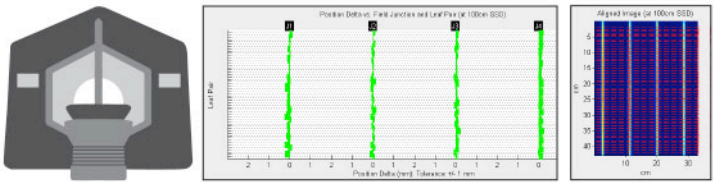

Varian® Halcyon™ MLC Analysis

RIT software is now compatible for verification and quality assurance of Varian Halcyon machine MLCs, used for image-guided radiation therapy (IGRT). Easily perform MLC QA, including a picket fence analysis of the Halcyon machine, which features a dual-layer multi-leaf collimator.

RapidArc® is not yet supported for the Halcyon™.

Cerberus Hands-Free Phantom Analysis

Cerberus, is our hands-free phantom analysis automation tool that operates in the background of your machine. Cerberus now allows you to sort with up to four DICOM tags, which it can use to select and process incoming files.

RunQueueC Preference & Tolerance Customization

When performing batch phantom analysis with RunQueueC, customize your preference profile and tolerances. Your customized profiles can be loaded directly from the interface, allowing you to easily select a profile for an analysis report specific to your machine.

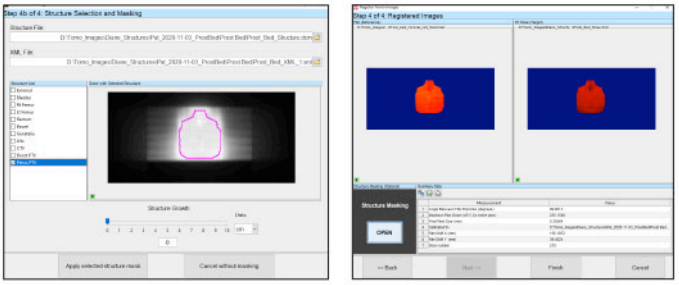

TomoTherapy® Registration Structure Analysis

RIT's TomoTherapy Registration analysis now allows a structure to display as an overlay ROI. Any structure in the Accuray Precision® plan can be used (e.g. PTV), and RIT software is compatible with Accuray's latest treatment planning system. Now, your analysis can be limited to the structure of your choosing, plus a user-defined margin, if you prefer. Then, use RIT's Patient QA routines to measure your results (Gamma, Subtraction, DTA, or one of 28 other analysis routines) within the ROI.

TomoTherapy® TG-148 Machine QA

The analysis routines for Static Gantry Angle and Helical Gantry Angle have been revised to improve the rotational invariance. The Overhead Laser routine can now handle smaller films, and a full 8x10 film is no longer required.

Optimized CIRS 062x Phantom Analysis

RIT's expanded CIRS 062x phantom analysis capability now covers most 062x phantoms (062, 062A, and 062M). The instant, one-click analysis now supports electron density analysis of the metal plugs and easy modification of the material values tolerances.

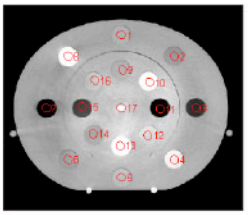

CLICK TO SEE ALL THE NEW UPDATES

RIT®

RADIMAGE.COM

+1.719.590.1077, Opt. 4 // sales@radimage.com // Connect with RIT on social media @RIT4QA

Received: 20 October 2021 | Revised: 11 January 2022 | Accepted: 26 January 2022

DOI: 10.1002/mp.15505

RESEARCH ARTICLE

MEDICAL PHYSICS

Increase of the transmission and emittance acceptance through a cyclotron-based proton therapy gantry

Vivek Maradia[1,2] | **Anna Chiara Giovannelli**[1,2] | **David Meer**[1] | **Damien Charles Weber**[1,3,4] | **Antony John Lomax**[1,2] | **Jacobus Maarten Schippers**[5] | **Serena Psoroulas**[1]

[1] Center for Proton Therapy, Paul Scherrer Institute, Villigen, Switzerland

[2] Department of Physics, ETH Zurich, Villigen, Switzerland

[3] Department of Radiation Oncology, University Hospital Zurich, Zurich, Switzerland

[4] Department of Radiation Oncology, University Hospital Bern, University of Bern, Bern, Switzerland

[5] Large Accelerator Facility, Paul Scherrer Institute, Villigen, Switzerland

Correspondence
Vivek Maradia, Center for proton therapy, Paul Scherrer Institute, Switzerland.
Email: vivek.maradia@psi.ch

Funding information
PSI's CROSS funding scheme; Swiss National Science Foundation, Grant/Award Number: 185082

Abstract

Purpose: In proton therapy, the gantry, as the final part of the beamline, has a major effect on beam intensity and beam size at the isocenter. Most of the conventional beam optics of cyclotron-based proton gantries have been designed with an imaging factor between 1 and 2 from the coupling point (CP) at the gantry entrance to the isocenter (patient location) meaning that to achieve a clinically desirable (small) beam size at isocenter, a small beam size is also required at the CP. Here we will show that such imaging factors are limiting the emittance which can be transported through the gantry. We, therefore, propose the use of large beam size and low divergence beam at the CP along with an imaging factor of 0.5 (2:1) in a new design of gantry beam optics to achieve substantial improvements in transmission and thus increase beam intensity at the isocenter.

Methods: The beam optics of our gantry have been re-designed to transport higher emittance without the need of any mechanical modifications to the gantry beamline. The beam optics has been designed using TRANSPORT, with the resulting transmissions being calculated using Monte Carlo simulations (BDSIM code). Finally, the new beam optics have been tested with measurements performed on our Gantry 2 at PSI.

Results: With the new beam optics, we could maximize transmission through the gantry for a fixed emittance value. Additionally, we could transport almost four times higher emittance through the gantry compared to conventional optics, whilst achieving good transmissions through the gantry (>50%) with no increased losses in the gantry. As such, the overall transmission (cyclotron to isocenter) can be increased by almost a factor of 6 for low energies. Additionally, the point-to-point imaging inherent to the optics allows adjustment of the beam size at the isocenter by simply changing the beam size at the CP.

Conclusion: We have developed a new gantry beam optics which, by selecting a large beam size and low divergence at the gantry entrance and using an imaging factor of 0.5 (2:1), increases the emittance acceptance of the gantry, leading to a substantial increase in beam intensity at low energies. We expect that this approach could easily be adapted for most types of existing gantries.

KEYWORDS
efficient treatment delivery, FLASH, gantry beam optics, high dose rates, proton therapy gantry

1 | INTRODUCTION

Over the past two decades, particle therapy is experiencing significant development. The most advanced and most used dose delivery method is pencil beam scanning (PBS).[1] However, its use is limited in the case of moving tumors due to dose delivery corruption caused by motion during treatment. To treat moving targets such as lung or liver tumors effectively and efficiently, it is required to use motion mitigation techniques such as breath-hold,[2,3] rescanning,[4] and gating.[5] To minimize the breath-hold duration, a treatment unit is ideally required, that can provide both high-intensity beams (to reduce beam-on time) and fast energy changes (to reduce dead-times). High-intensity beams could increase the patient comfort during the treatment by reducing treatment delivery time. It could also help in increase of patient throughput. In addition, rescanning and gating could both also be more effective if one could use a large beam size (to reduce the interplay effect)[6] with high-intensity beams, whilst higher intensities will also permit a more efficient delivery of hypofractionated treatments and will be an important pre-condition for proton ultra-high dose rate (i.e., FLASH) irradiations. On the other hand, dose conformity will be compromised if the beam size is too large. Thus, to achieve a combination of high-intensity beams together with different beam sizes at the isocenter, new developments are needed in the currently used cyclotron-based proton/ion therapy machines (i.e., the majority of PBS treatment facilities).

One of the main components of the proton therapy delivery system is the gantry (rotating beamline). Over the years, many different types of gantries have been designed for proton therapy. For cyclotron-based proton therapy facilities, and for low energy beams, the beam emittance after the energy degrader is typically to be in the order of a few hundred π*mm*mrad.[7] In fact, the emittance accepted by the gantry determines the maximum emittance that is transported through the fixed beamline between the cyclotron and the gantry, and hence also affects the achievable beam intensity at the isocenter. A gantry's emittance acceptance is determined by both the gantry beam optics and the beam phase space at the coupling point (CP), whilst the imaging factor obtained in the beam optics of the gantry, together with the beam phase space at the CP,[7–9] determine the beam size at isocenter. In this work, we have investigated how improvements on the emittance acceptance and imaging factor can achieve improved beam intensities (dose rates) at the isocenter, whilst also allowing for a range of beam sizes.

Conventional beam optics of cyclotron-based proton gantries were designed to provide point-to-point focusing in both planes, with an imaging factor of between 1 and 2 from the CP to isocenter.[10,11] As such, a factor 1-2 smaller beam size at the CP is required to achieve a small beam size at the isocenter. Due to the typically used beam emittances of $\leq$30 π*mm*mrad, this, in turn, results in large beam divergences (angular spread within the beam) in the gantry, increasing the possibility of beam losses along the gantry as the beam envelope approaches the beam pipe. For instance, for PSI's Gantry 2, by transporting 30 π*mm*mrad emittance (3 mm beam size and 10 mrad divergence at the CP) with 1:1 imaging, a transmission of 57% is achieved for lower energies (70–100 MeV)[7,8] (transmission through the gantry is defined as the ratio of beam current at isocenter to the beam current at the CP). However, to achieve higher intensity for lower energy beams, it is desirable to transport a higher emittance through both the beamline and gantry. In this article, we report on a new beam optics approach which transports larger emittances through the gantry. For this, we propose to use an imaging factor of 0.5 (= 2:1 imaging) between the CP and isocenter together with a larger beam size and lower divergence at the CP, thus maximizing transmission through the gantry. Additionally, we propose the use of a collimator stack at the CP to achieve a range of beam sizes at the isocenter without making any changes in gantry or beam optics. Finally, we show the effect of momentum spread on beam transmission through the gantry, since this increases significantly at lower energies due to scattering in the degrader. As most gantries use similar beam optics, we expect the method described in this paper to be applicable to other gantries as well.

2 | METHODS

The new beam optics for the gantry was first developed and designed using TRANSPORT[12] calculations, then verified and investigated using MC simulations, and finally validated in experimental measurements on Gantry 2 at PSI.

For all simulations and measurements in this study, we have used a 90 MeV proton beam. However, as all magnet settings can just be scaled as a function of momentum, the optics solutions presented here are valid for all energies and will only depend on the initial emittance and orientation of the phase space. In addition, the optics developed here only use modified quadrupole magnet field strengths and, apart from the collimator at CP, no mechanical modifications have been assumed. In the following, all beam sizes, divergences, and emittances are expressed as 2-sigma values.

2.1 | Effect of initial beam phase space on transmission

The beam optics discussed in this article is based on an optimization of the orientation of the beam's phase space at the gantry entrance. To demonstrate the effect

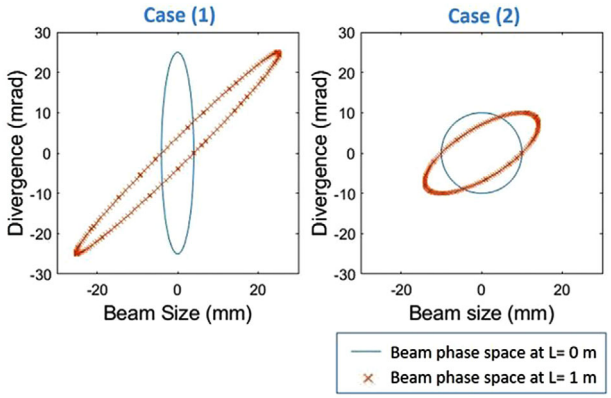

FIGURE 1 Evolution of the phase space in transverse plane from the start until the end of a 1 m long beam pipe (beam emittance is 100 π*mm*mrad)

of the initial phase space on transmission through the beam pipe, we apply two different starting conditions to transport 100 π*mm*mrad emittance through a 1 m long beam pipe with a radius of 20 mm. Two different orientations of the initial beam phase space have been selected at $L = 0$ m (Figure 1). In case (1), the beam size increases rapidly as a function of length, due to the initial large divergence. After a drift of $L = 1$ m, it is larger than the beam pipe radius and initiate beam losses. However, in case (2), although the initial beam size is larger, the initial divergence is smaller in order to preserve the same emittance. Due to this smaller divergence, the beam size remains smaller than the beam pipe radius, even after 1 m. In addition, this increased beam size only marginally contributes to the beam size along the 1 m drift in the beam pipe.

Therefore, applying this method, the transmission through the gantry could be maximized by using a large beam size and low divergence beam at the CP.

2.2 | Beam optics design

To avoid the influence of beam energy and gantry rotation angle on both beam size at isocenter and beam transmission through the gantry, in this study, we assume the following boundary conditions:

- Same beam size and same divergence at the CP in both transverse planes (in terms of the sigma matrix describing the beam properties in a matrix formalism, $\sigma 11 = \sigma 33$ and $\sigma 22 = \sigma 44$).
- Point-to-point imaging in the transport system between CP and isocenter (in terms of transfer matrix R12 = 0 and R34 = 0).
- Full achromaticity of the transport system (R16 = R26 = 0).
- Equal magnifications in both transverse planes of imaging from CP to Isocenter (R11 = R33 and R22 = R44).

TABLE 1 Beam parameters (2-sigma values) at the CP with different imaging factors while transporting 100 π*mm*mrad emittance through the gantry

	Beam size (mm)	Divergence (mrad)	Imaging factor
Case (a)	8	12.5	1:1
Case (b)	10	10	1.25:1
Case (c)	12	8.33	1.5:1
Case (d)	14	7.14	1.75:1
Case (e)	16	6.3	2:1

The matrix formalism code TRANSPORT[12] has been used to design the new beam optics, based on the design of Gantry 2 here at PSI.[10] To study the effect of CP beam phase space on the emittance acceptance of the gantry and transmission, we modified the input beam phase space (beam size, divergence, and emittance) and adjusted the optics under the above-mentioned conditions, with the beam being imaged from the CP to the isocenter with the aim to achieve an 8 mm beam size at the isocenter for different CP beam sizes ranging from 8 to 16 mm. The resulting imaging factor required for each scenario ranges from 1:1 to 2:1 (shown in Table 1).

Due to energy straggling in the degrader, the momentum spread for low energy beams is large, resulting in considerable beam losses at the apertures of magnets and beam pipe. For this reason, low energy beam intensities are proportional to the accepted momentum band. As such, the beam optics have been designed so that achromaticity was achieved in all cases. In this way, a large momentum band ($\Delta p/p = \pm 1\%$) can be transported through the gantry without increasing the isocenter spot size due to dispersion.

2.3 | Monte Carlo simulations

To calculate the transmission through the gantry, we used the BDSIM 1.4.1[13] Monte Carlo simulation toolkit. For this, we built a model of PSI's Gantry-2 in BDSIM (as shown in Figure 2) based on recommended modules for proton therapy (*G4EmStandardPhysics_option4, G4HadronPhysicsQGSP_BIC_HP, G4StoppingPhysics, G4HadronElasticPhysicsHP, and G4EmStandardPhysicsWVI*) which has been benchmarked against measurements.[7] A sensitivity analysis of the BDISM simulation was also performed using different electromagnetic models like *G4EmStandardPhysics_option0-3*.

For the BDSIM simulations, we have assumed vacuum beamlines until the exit of the last bending magnet D3 (see Figure 2). From there on, the beam goes through the air and all nozzle components, such as beam monitors. To minimize the statistical uncertainty,

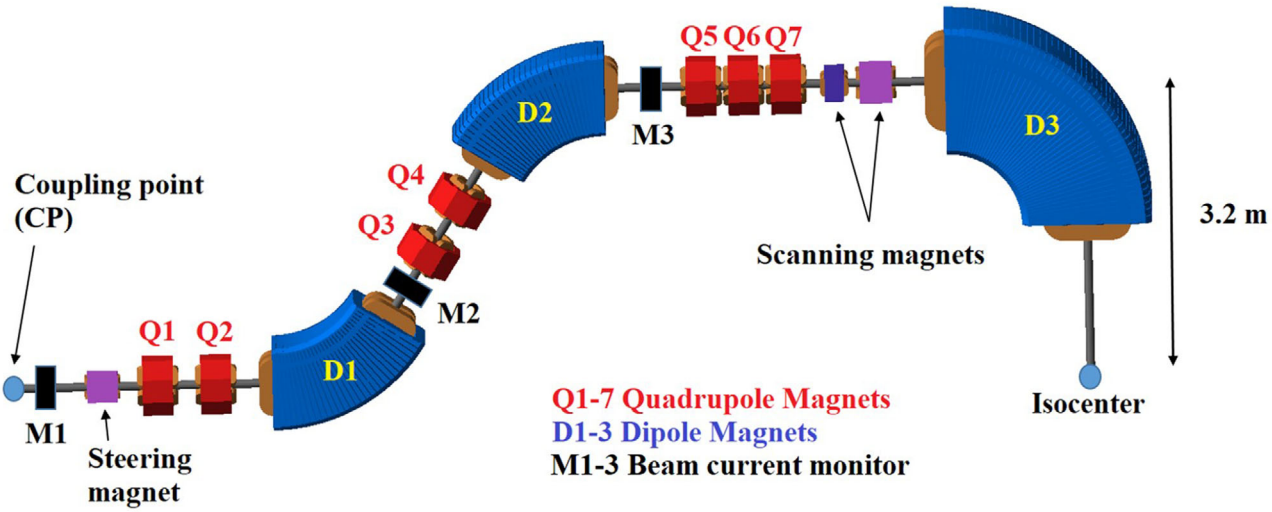

FIGURE 2 PSI's Gantry 2 layout in BDSIM

for each simulation, we used 10 million particles. Post-processing of the simulation data has been performed using ROOT v6.22 and MATLAB v9.6 scripts.

2.4 | Measurement setup

Experimental verification of the proposed beam optics has been performed on PSI's Gantry 2. The beamline from the cyclotron to the CP can transport a maximum of 60 π*mm*mrad in X-plane and 130 π*mm*mrad in the Y-plane. In order to investigate transport of emittance up to 120 π*mm*mrad through gantry, a 30 μm thick tantalum scatter foil has been inserted after the energy selection system, which increases the emittance in both planes up to 135 π*mm*mrad emittance. In addition, different beam sizes entering the gantry can be defined by selecting different fixed aperture collimators positioned at the gantry entrance (CP). For this experiment, we used fixed copper collimators with a radius of 20 mm and inserts with radius ranging from 4 to 16 mm (Figure 3). The inserts have a step on the outside to prevent possible proton leakage between the insert and fixed aperture collimator. To select the different divergences at the CP, the field strength of the last quadrupole triplet in the beamline, 2.3 m before the CP (not shown in Figure 2) was adjusted.

Transmission through the gantry was measured with three current monitors on the gantry (M1-3, see Figure 2).[14] In addition, to estimate the beam current at the nozzle exit, the clinically relevant dose monitor (ionization chamber), positioned in the nozzle, was used. The distance of the isocenter from the nozzle is about 70 cm. The beam intensity coming out of the CP collimator was measured with monitor M1 (see Figure 2).

FIGURE 3 Fixed copper collimator with a diameter of 40 mm and additional inserts with different radius ranging from 4 to 16 mm

3 | RESULTS

Here we will discuss the results of our calculations and compare them with measurements. We will start with a study of the effects of the variation of the *orientation* of the beam's phase space at the CP on gantry transmission. Then the effect of the initial emittance *magnitude* on gantry transmission and the effect of *momentum spread* in the initial beam will be discussed. We also discussed the effect on *beam size* at isocenter as a function of beam size at CP

3.1 | Effect of beam phase space at CP on gantry transmission

To study the effect of beam phase space at CP on gantry transmission, we chose five different phase space

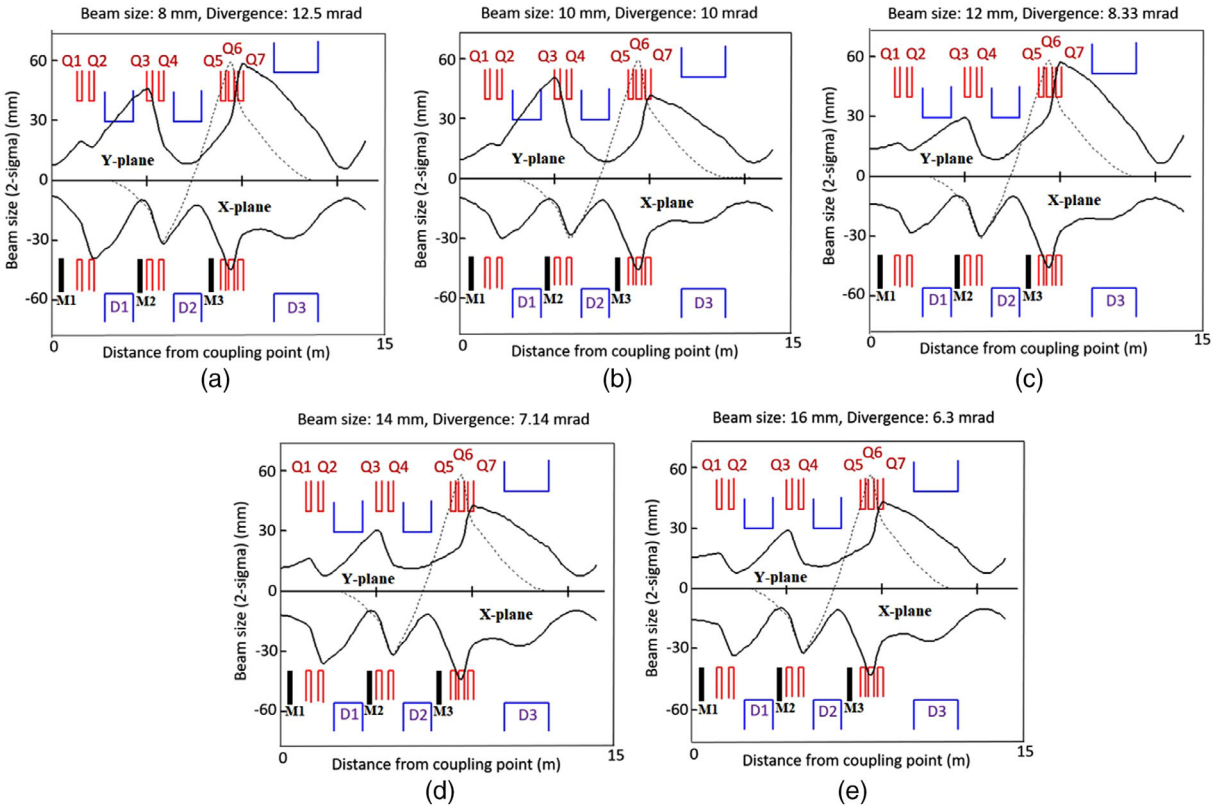

FIGURE 4 Gantry beam optics to transport 100 π*mm*mrad with different beam phase space at the CP. The beam envelopes show the beam size in 2-sigma values and the dispersion (dashed line) along PSI's Gantry 2 beamline (the lower half of each figure shows beam envelope in X-plane (bending plane) and the upper half shows envelope in Y-plane). Figure (a), (b), (c), (d), and (e) represents 1:1, 1.25:1, 1.5:1, 1.75:1, and 2:1 imaging, respectively. Elements D = dipole magnets and elements Q = quadrupole magnets. The dispersion only occurs in the bending plane (in our case, X-plane)

orientations of which each had the same 100 π*mm*mrad emittance. The gantry beam optics were then modified for all five cases to transport this same emittance through the gantry. In order to achieve the same beam size at the isocenter, however, beam optics with different magnification factors, depending on the beam size at CP, were designed. Table 1 shows the selected beam size and divergence at CP, together with the resulting imaging factor for five different beam widths, whereas Figure 4 shows their beam envelopes through the gantry. A ±1% momentum spread ($\Delta p/p$) was assumed for all cases. Due to the large dispersion, some beams were inevitably lost in the quadrupole triplet in all the cases.

When transporting beams with 100 π*mm*mrad emittance through the gantry, we get a minimum transmission of about 40% for a beam size of 8 mm and large divergence (12.5 mrad) (Figure 5a). By increasing the beam size and decreasing the divergence, however, we see a gradual increase in transmission through the gantry, reaching a maximum transmission of about 60%, for the largest beam size at CP (16 mm), corresponding to the smallest divergence. This matches expectations as can be observed in Figures 4 and 5b. This improvement in transmission results from substantially less beam loss in the first two quadrupole and dipole magnets as the beam envelopes are now far from the apertures of these magnets for case (d) and (e) compared to cases (a)–(c). As such, and combined with a 2:1 imaging, we get a maximum transmission through the gantry. Nevertheless, due to the maximal effect of the dispersion in the quadrupole triplet, it is still unavoidable to have some beam losses due to the 1% momentum spread.

3.2 | Effect of initial emittance on gantry transmission

Here, we study the transport of different emittances through the gantry while having the same imaging and same beam size at CP. Figure 6a shows the measured and simulated transmission data for different emittances transported through gantry using 2:1 imaging while keeping the same beam size (16 mm) at the CP and varying the divergence of the beam. For an emittance of 60 π*mm*mrad, we achieve the highest (~70%) transmission through gantry as this has the smallest divergence (3.8 mrad) of all compared scenarios. However, if the divergence increase (Figure 6b), the beam is lost in the first two quadrupoles and dipole

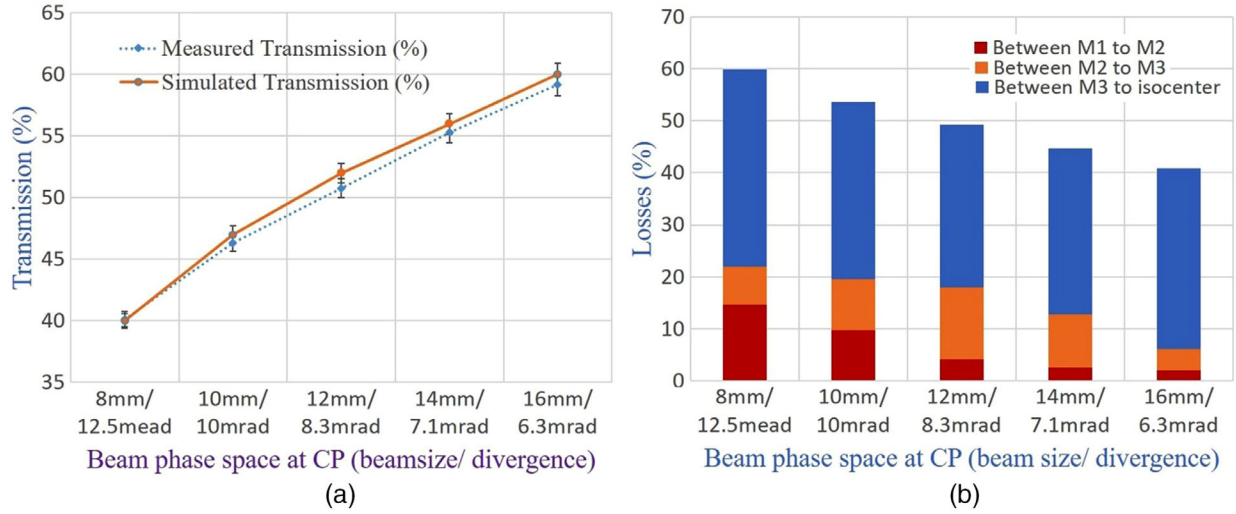

FIGURE 5 (a) Beam transmission through gantry (simulation and measured) for transporting 100 π*mm*mrad through gantry with different beam parameters at the CP with different imaging factors as shown in Figure 4. (b) Beam losses distribution (measured) along the different parts of the gantry while transporting 100 π*mm*mrad emittance with different phase space at the CP

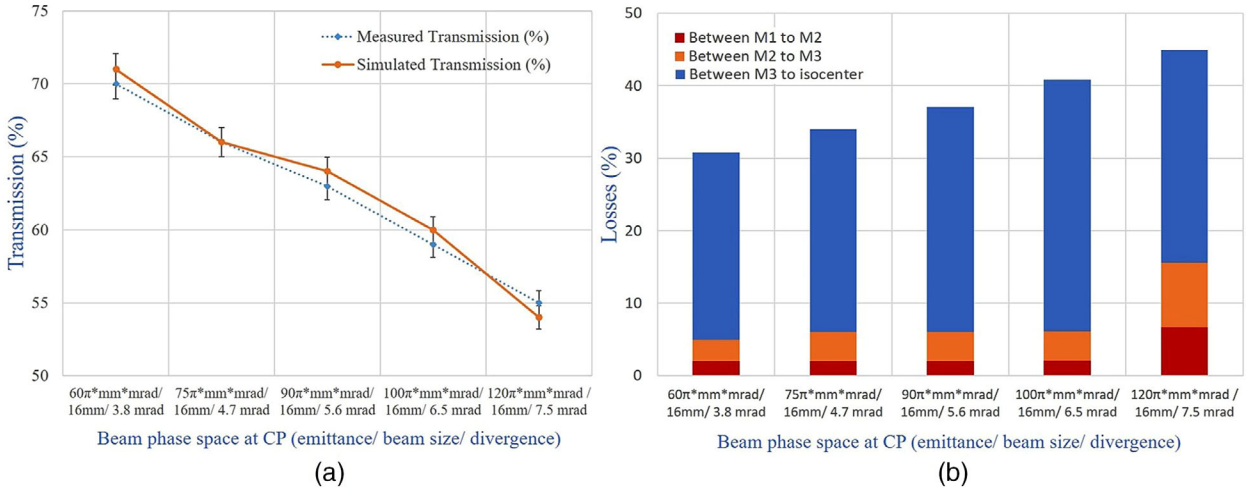

FIGURE 6 (a) Transmission calculation (simulation and measured) by transporting different emittances through gantry with 16 mm (fixed) beam size and different divergence values at the CP. (b) Beam losses distribution (measured) along the different parts of the gantry while transporting different emittances through gantry with 16 mm (fixed) beam size and different divergence values at the CP. For all cases, the beam optics is designed with 2:1 imaging

magnets. Hence, for a fixed beam size at CP, increasing emittance/divergence decreases transmission, with the lowest transmission (54%) corresponding to an emittance of 120 π*mm*mrad with a 7.5 mrad divergence. In contrast, however, using a large beam size (16 mm) and low divergence (7.5 mrad) at CP, which increases the emittance by a factor of 2, the decrease in the transmission is only 15% (Figure 6a).

3.3 | Beam size at isocenter as a function of beam size at CP

Figure 7 shows the change in measured beam size at the isocenter as a function of the beam size at the CP. For all scenarios, a beam divergence of 6 mrad and 2:1 imaging was used with the beam size at the CP being changed using collimators with different apertures (see Figure 3). For all scenarios, a momentum spread of 1% has been used.

Figure 7 shows that the measured and BDSIM simulated beam sizes at the isocenter have been found to be more or less linearly dependent on the beam size at the CP. However, the effective magnification factor decreases somewhat moving from beam sizes at CP of 2.75 to 1.03. This is caused by multiple scattering in the vacuum window, air, and nozzle components[15] following the last bending magnet D3. It can be observed that similar beam sizes are predicted by BDSIM and TRANSPORT (Figure 7) if the gantry beamline is assumed to

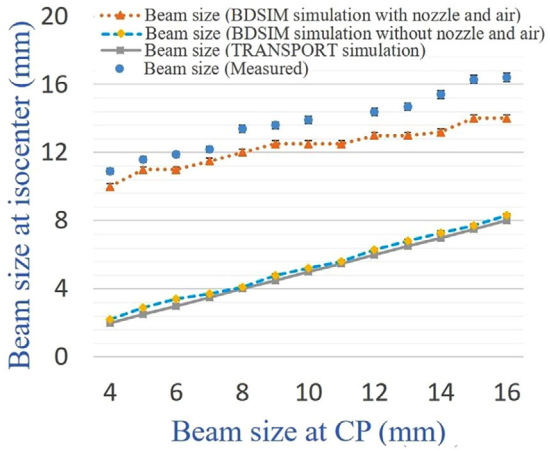

FIGURE 7 Measured and simulated (BDSIM and TRANSPORT simulation) beam size at isocenter by using 6 mrad (fixed) divergence and different beam sizes at the CP. Beam sizes are in 2-sigma values

be in a vacuum and the nozzle is ignored. It is important to note that in that case, the beam size at the isocenter is not affected by the losses in the gantry but only depends on the imaging factor. When adding the air and nozzle components, however, the additional beam scattering inevitably increases the beam size at the isocenter. It is therefore not possible to get perfect imaging in practice. Nevertheless, we are still able to vary the beam size at the isocenter by adjusting the collimator at CP.

3.4 | Effect of momentum spread on gantry transmission

As shown in Figure 5a, for a momentum spread of $\Delta p/p = \pm 1\%$, the highest transmission of 60% has been obtained for a beam divergence of 6.3 mrad and a beam size of 16 mm at CP. Nevertheless, due to the large effect of the dispersion in the quadrupole triplet, however, also in this situation beam losses occur. As such, in this final study, we have investigated the effect of momentum spread on transmission through the gantry based on these "best performing" optics.

As can be deduced from Figure 8a, most beam losses due to momentum spread occur in the X-plane of the triplet, with some additional losses in Q4. Figure 8b shows the transport through the gantry at a smaller momentum spread ($\Delta p/p$ of 0.6%). As would be expected, the losses decrease with this reduced momentum spread. Figure 9a shows the transmission as a function of momentum spread from 0.6 to 1.1% $\Delta p/p$, with 0.6% $\Delta p/p$ being the smallest momentum band used in treatments (i.e. that for 70 MeV). For this momentum band, we achieved the maximum transmission of 76%, whereas, for a $\Delta p/p = \pm 1.1\%$, transmission reduced to 50%. As shown in Figure 9b, for all cases, the losses between M1 and M3 (= losses in Q4) remain the same, but beam losses increase between M3 and isocenter for the larger momentum bands, due to losses in the quadrupole triplet. The fact that the losses in Q4 depend less on dispersion as expected from its relatively large value, is due to the fact that the monochromatic beam size at that location is already big and mostly determined by the imaging to that point. Since the beam size is already large, dispersion and momentum spread have a small additional contribution. In the triplet, however, the beam size for a monochromatic beam is small, with the momentum spread being the main determinate of beam size, due to the large dispersion at this location.

4 | DISCUSSION

In this work, we have demonstrated that, for a fixed value of emittance, we could maximize transmission through the gantry by using a large beam size and low divergence beam at the CP (as shown in Figures 5a and 1, respectively).

This improvement in transmission comes from the reduction of losses in the first quadrupole doublet and dipole magnet (as shown in Figures 5b and 4e, respectively.). This is due to the smaller divergence of the beam at CP. However, this has enabled us to increase the beam size at CP, so that a larger emittance can be transported through the gantry. Here, we showed transmission improvement results for the 90 MeV beam. However, as the beam optics design is energy independent, for the same emittance and momentum spread value, we will get the same transmission for all energy beams. The improvement in transmission reported here is, however, dependent on the emittance acceptance of the PSI Gantry 2. However, the first section of the gantry, which matches the incoming beam to the dipole entry, is similar for all types of gantries, being a combination of a drift beam pipe and/or quadrupole magnet. Hence, the use of a large beam size and low divergence beam at the CP, along with 2:1 (or any demagnification) imaging could bring an improvement in transmission for all types of gantries.

To achieve 2:1 imaging, the beam must be strongly focused to the isocenter using the last quadrupole doublet/triplet of the gantry. Some commercial solutions use two bending magnets for this, requiring a very large last bending magnet. In this case, the distance between the last quadrupole doublet/triplet to the isocenter is relatively large compared to gantries with three bending magnets (like PSI's Gantry 2). Because of this, gantries with two bending magnets may not be able to focus the beam strongly enough. Nevertheless, even in this case, transmissions could be partially increased, even if less demagnification is possible.

We have also demonstrated that by using a large beam size and low divergence beam at the CP, we could achieve reasonably high (>50%) transmission

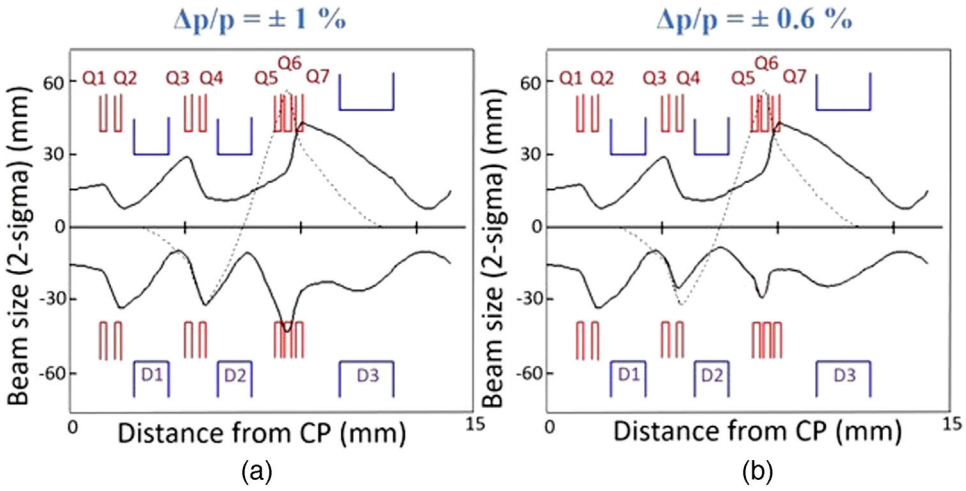

FIGURE 8 Gantry beam optics to transport 100 π*mm*mrad (16 mm beam size and 6.3 mrad divergence at CP). (a) Beam optics with $\Delta p/p = \pm 1\%$ and (b) beam optics with $\Delta p/p = \pm 0.6\%$. The dispersion only occurs in the bending plane (in our case, X-plane)

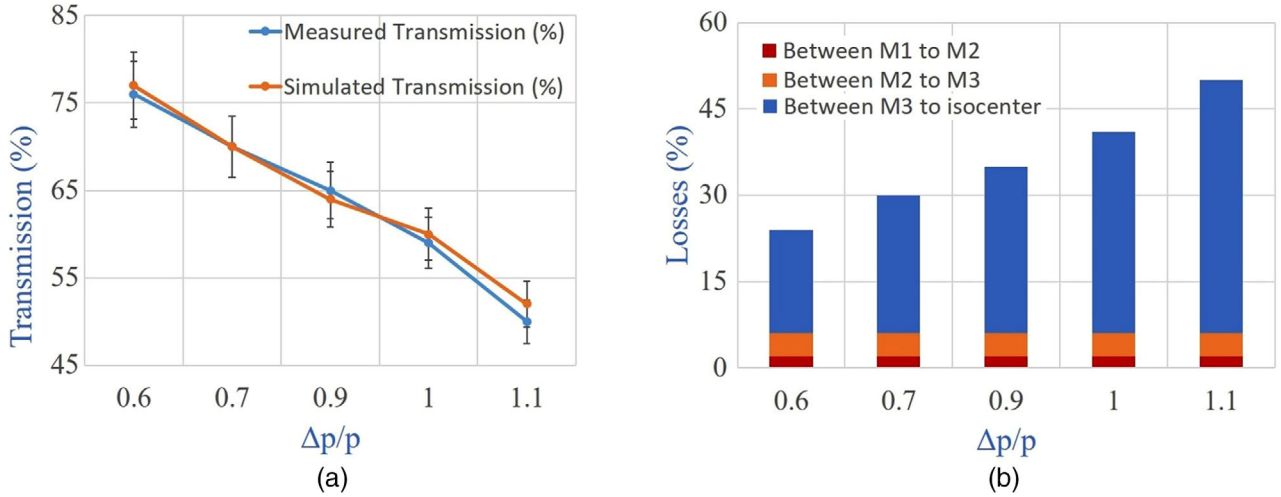

FIGURE 9 (a) Effect of $\Delta p/p$ on gantry transmission. 100 π*mm*mrad emittance was transported through gantry with 16 mm beam size and 6.3 mrad divergence at the CP with 2:1 imaging. For all the cases, we used the same beam optics. (b) Beam losses distribution (measured) along the different parts of the gantry while transporting 100 π*mm*mrad emittance (16 mm bema size and 6.3 mrad divergence at the CP) with 2:1 imaging

even for the high emittance (120 π*mm*mrad) as shown in Figure 6a. Currently, most gantries transport 30 π*mm*mrad or less emittance through the gantry. However, we have shown in another study that the transport of 100 π*mm*mrad emittance in both transversal planes could bring an increase in overall transmission (cyclotron to isocenter) by almost a factor 6 compared to transporting 30 π*mm*mrad for low energy beams.[7] Therefore, the solution shown in this article, together with larger emittance transported from the cyclotron to the CP, could strongly enhance the beam currents reached at isocenter in cyclotron-based gantries.

One limitation of the higher emittance could be the associated larger beam size at the isocenter. With increased emittances transported through the gantry, the beam size at the isocenter will increase, since it is not possible to obtain a stronger demagnification in the existing gantry. However, for the gantry studied in this work, the beam sizes obtained experimentally (shown in Figure 7) are not that different from the beam sizes used clinically and therefore we do not see this as a strong clinical limitation in the applicability of the technique.[16,17] If a larger beam size with high-intensity beams could help achieve field delivery times similar to typically achievable breath-hold durations, such degraded lateral penumbras will likely be compensated for by a substantial reduction of size of the internal target volume (IVT) typically required to ensure target coverage. In addition, a larger beam size could be of benefit for reducing the required number of spots in the

treatment planning, reducing dead times, and therefore also additionally shortening treatment times. Further studies are necessary to demonstrate the clinical usability of the large beam size beams.

As shown in Figure 7, we demonstrated that by having a 2:1 imaging of the beam optics we could achieve different beam sizes at the isocenter independently of the gantry rotation and the gantry beam optics just by changing the beam size at the CP. To select different beam sizes at the CP, we could use a movable collimator array with different aperture sizes. As such, we plan to investigate the possibility to use different beam sizes for the treatment of a tumor, by using large beam sizes, with increased transmission, for the inner part of the tumor and small beam sizes for the outer part of the tumor in order to shorten the treatment delivery time while sparing surrounding healthy tissues.

Finally, we have also demonstrated that for a fixed emittance value, the transmission through the gantry would increase by reducing the $\Delta p/p$ of the beam (as shown in Figure 9a). Momentum band define the lateral margins of the beam (penumbra). Smaller the value of $\Delta p/p$, the sharper the penumbra. When we reduce the momentum band of the beam (as shown in Figure 8), the beam size at the quadrupole triplet (Q5–7) of the gantry will reduce, since there the beam size is mostly determined by the large dispersion at that location. This will reduce losses in the triplet. Although the distal fall-off of the dose distribution has some dependence on the momentum spread used, the momentum spectrum at the isocenter is expected to have a negligible change due to these losses as they will only occur in the tails of the momentum distribution. In this respect, it is important that, due to the achromatic beam optics, the lateral beam size at the isocenter is independent of the momentum spread of the beam.[18] As such it would make it interesting to add the momentum spread as one of the parameters to be optimized in the treatment planning.

5 | CONCLUSION

In summary, we have shown that for a fixed emittance value, it is possible to maximize proton beam transmission through a gantry by using a small divergence value and large beam size at the coupling point (CP), together with de-magnifying beam optics imaging from CP to the isocenter. Additionally, we have shown that the use of large beam sizes and low divergence at the CP allows the transport of larger emittances through the gantry while achieving reasonable transmission (>50%) of even low energy beams through the gantry. By transporting 100 π*mm*mrad emittance through the beamline and gantry, it is possible to achieve almost 6 nA beam current (800 nA from cyclotron) at the isocenter for 70 MeV beam in combination with asymmetric emittance selection collimators.[7] In addition, the studied beam optics with point-to-point imaging gives the flexibility to change the beam size at the isocenter, without changing the gantry beam optics simply by adjusting the beam size at the CP. Such achromatic optics allow beam transport with different momentum spread so that in treatment planning one can balance intensity against fall-off of the dose distribution.

These new beam optics could give the flexibility to choose different beam sizes and intensities of the beam based on the clinical requirement without making a significant change in the beamline or gantry. It could reduce the difficulties to treat moving tumors and could enable the treatment with certain motion mitigation techniques efficiently and effectively. High intensity could allow to deliver a field within a single breath-hold.[19,20] It could also help to reach the dose rates required for FLASH irradiations. Altogether, this will increase the possibilities to treat new indications in current and future proton therapy facilities.

ACKNOWLEDGMENTS

We thank Dr. Rudolf Doelling, Dr. Christian Baumgarten, and Dr. Robert Michael Schäfer for their support during the measurements. We acknowledge the help of the PSI cyclotron operation group, PSI vacuum group, and PSI radiation protection group. Open access funding provided by ETH-Bereich Forschungsanstalten. WOA Institution: ETH-Bereich Forschungsanstalten.

CONFLICT OF INTEREST

The authors declare no conflict of interest.

DATA AVAILABILITY STATEMENT

The data will be available to interested researches upon request and under a confidentiality agreement, as they contain sensitive information about a PSI product.

REFERENCES

1. Pedroni E, Bacher R, Blattmann H, et al. The 200-Mev proton therapy project at the Paul Scherrer Institute: conceptual design and practical realization. *Med Phys*. 1995;22(1):37-53. https://doi.org/10.1118/1.597522
2. Hanley J, Debois MM, Mah D, et al. Deep inspiration breath-hold technique for lung tumors: the potential value of target immobilization and reduced lung density in dose escalation. *Int J Radiat Oncol Biol Phys*. 1999;45(3):603-611. https://doi.org/10.1016/S0360-3016(99)00154-6
3. Dueck J, Knopf AC, Lomax A, et al. Robustness of the voluntary breath-hold approach for the treatment of peripheral lung tumors using hypofractionated pencil beam scanning proton therapy. *Int J Radiat Oncol Biol Phys*. 2016;95(1):534-541. https://doi.org/10.1016/j.ijrobp.2015.11.015
4. Schätti A, Zakova M, Meer D, Lomax AJ. Experimental verification of motion mitigation of discrete proton spot scanning by re-scanning. *Phys Med Biol*. 2013;58(23):8555-8572. https://doi.org/10.1088/0031-9155/58/23/8555
5. Ohara K, Okumura T, Akisada M, et al. Irradiation synchronized with respiration gate. *Int J Radiat Oncol Biol Phys*. 1989;17(4):853-857. https://doi.org/10.1016/0360-3016(89)90078-3
6. Paganetti H, Henning W, Choi N, et al. Motion interplay as a function of patient parameters and spot size in spot scanning proton therapy for lung cancer. *Int J Radiat Oncol Biol Phys*.

2014;86(2):380-386. https://doi.org/10.1016/j.ijrobp.2013.01.024. Motion
7. Maradia V, Meer D, Weber DC, Lomax AJ, Schippers JM, Psoroulas S. A new emittance selection system to maximize beam transmission for low-energy beams in cyclotron-based proton therapy facilities with gantry. *Med Phys*. 2021;48(12):7613-7622. https://doi.org/10.1002/mp.15278
8. Maradia V, Meer D, Giovannelli, et al. A novel beam optics concept to maximize the transmission through cyclotron-based proton therapy gantries. *Proc IPAC2021*. 2021:2477-2479. https://doi.org/10.18429/JACoW-IPAC2021-TUPAB407
9. Maradia V, Meer D, Giovannelli AC, et al. New gantry beam optics solution for minimizing treatment time in cyclotron-based proton therapy facilities. In: *PTCOG 2021 Conference*. Particle Therapy Co-Operative Group; 2021. https://doi.org/10.3929/ethz-b-000497120
10. Pedroni E, Meer D, Bula C, Safai S, Zenklusen S. Pencil beam characteristics of the next-generation proton scanning gantry of PSI: design issues and initial commissioning results. *Eur Phys J Plus*. 2011;126(7):1-27. https://doi.org/10.1140/epjp/i2011-11066-0
11. Yves J. Gantry comprising beam analyser for use in particle therapy - US 9,289,624 B2 - PatentSwarm. 2010:1-11. https://patentswarm.com/patents/US9289624B2. Accessed: 13 May 2021.
12. Brown KL, Carey DC, Iselin FC, Rothacker F. Transport, a Computer Program for Designing Charged Particle Beam Transport Systems. CERN; 1980. https://doi.org/10.5170/CERN-1980-004
13. Nevay LJ, Boogert ST, Snuverink J, et al. BDSIM: an accelerator tracking code with particle–matter interactions. *Comput Phys Commun*. 2020;252:107200. https://doi.org/10.1016/j.cpc.2020.107200
14. Dölling R. Profile, current, and halo monitors of the PROSCAN beam lines. 2004;732:244-252. https://doi.org/10.1063/1.1831154
15. Pedroni E, Bearpark R, Böhringer T, et al. The PSI Gantry 2: a second generation proton scanning gantry. *Z Med Phys*. 2004;14(1):25-34. https://doi.org/10.1078/0939-3889-00194
16. Almhagen E, Boersma DJ, Nyström H, Ahnesjö A. A beam model for focused proton pencil beams. *Phys Medica*. 2018;52:27-32. https://doi.org/10.1016/j.ejmp.2018.06.007
17. Shamurailatpam D, Manikandan A, Ganapathy K, et al. Characterization and performance evaluation of the first-proton therapy facility in India. *J Med Phys*. 2020;45(2):59-65. https://doi.org/10.4103/jmp.JMP_12_20
18. Giovannelli AC, Maradia V, Meer D, et al. Beam properties within the momentum acceptance of a clinical gantry beamline for proton therapy. *Med Phys*. 2022;1-15. https://doi.org/10.1002/mp.15449
19. Maradia V. Intensity-modulated proton therapy treatment delivery of locally advanced non-small-cell lung cancers within a single breath-hold. 2021. https://doi.org/10.3929/ethz-b-000515078
20. Maradia V, Bertschi S, Krieger M, et al. PO-1762 feasibility study to achieve hypofractionated IMPT PBS within a single breath-hold for lung cancer. *Radiother Oncol*. 2021;161:S1488-S1489. https://doi.org/10.1016/s0167-8140(21)08213-x

How to cite this article: Maradia V, Giovannelli AC, Meer D, et al. Increase of the transmission and emittance acceptance through a cyclotron-based proton therapy gantry. *Med Phys*. 2022;1-10. https://doi.org/10.1002/mp.15505